Electrochemistry of Conductive Polymers 38. Electrodeposited Poly(3,4-ethylenedioxy-thiophene) Studied by Current Sensing Atomic Force Microscopy

Dong-Hun Han, Jae-Woo Kim, and Su-Moon Park*

Department of Chemistry and Center for Integrated Molecular Systems, Pohang University of Science and Technology, Pohang, Gyeongbuk 790-784, Korea

Received: October 11, 2005; In Final Form: June 1, 2006

Electrical and morphological properties of poly(3,4-ethylenedioxythiophene) (PEDOT) thin films electrodeposited on gold-on-silicon electrodes by galvanostatic, potentiostatic, and potentiodynamic methods have been determined using current sensing atomic force microscopic experiments. Surface morphologies and vertical conductivities of PEDOT films were affected by the experimental parameters including the preparation method, the current density, the potential, and the potentiodynamic cyclic number. Band gaps obtained from current−voltage curves of dedoped PEDOT were in excellent agreement with those obtained from absorption spectra. When the film thickness was increased on the gold-on-silicon electrode, the topographic images were not very well defined due to the high roughness but conductivities increased significantly in all the galvanostatically, potetiostatically, and potentiodynamically grown PEDOT films.

Introduction

Conducting polymers have been attracting a great deal of attention thanks to their potential applications to electronic devices,[1] sensors,[2] corrosion protection,[3] and actuators.[4] Electrical characteristics of these polymers are of central interest for their applications to the practical devices.

3,4-Ethylenedioxythipohene (EDOT), which is a thiophene derivative with its 3- and 4-positions blocked by an ethylenedioxy group, was initially used to facilitate preparation of linear polythiophene for an enhanced conductivity and to obtain a soluble polymer without undesired α,β and β,β couplings.[5] PEDOT, which shows a very high conductivity and stability and is almost transparent in thin, doped films, has received attention since the 1990s.[5−7] Now PEDOT films show wide applications for, e.g., antistatic layers in photographic films, conducting layers in electroluminescent devices, organic field effect transistors, and hole injecting layers in polymeric light-emitting diodes and polymer photovoltaic cells.[5,6] Because of these wide applications, PEDOT has been commercialized with commercial names such as BAYTRON P (Bayer AG) and ORGACON (Agfa).

The current-sensing atomic force microscopy (CS-AFM) with its conducting tip allows not only the topographical and current images to be obtained simultaneously but also current−voltage (I/V) traces to be recorded on selected spots of the image, where one wants to study electrical characteristics on a nanometer scale. This technique has been applied to various nanostructures such as single molecules,[8] biomolecules,[9] carbon nanotubes,[10] self-assembled monolayers,[11] quantum dots,[12] and other nanostructures[13] because it allows easy and reproducible contacts to be made with various substances without having to use difficult lithographic processes. Thus, the CS-AFM has a number of advantages in studying electrical properties of conducting polymer films. Recently, we and other investigators used this technique successfully for studies of conducting polymer films of various doping levels, proving its usefulness in the studies of doping distributions by obtaining two-dimensional current images and nanoscale electrical properties by measuring the I/V characteristics.[14,15]

Despite a large number of studies reported in the literature,[5−7] both electrical and morphological studies of PEDOT films have not been reported in the literature, particularly on the nanoscale. In our present study, we focus on: (1) a better understanding of the changes in morphologies and electrical properties of PEDOT films prepared under various experimental conditions and (2) how the semiconductor characteristics obtained from I/V curves of the dedoped PEDOT film are related with those from its absorption spectra. We report rather interesting results that the vertical conductivities of the PEDOT films show significant increases upon increase in their thickness and the band gaps obtained by two different techniques, i.e., the I/V characteristics and absorption spectroscopic measurements, show excellent agreement with each other.

Experimental Section

Acetonitrile (ACN, Aldrich, 99.8%, anhydrous) and 3,4-ehtylenedioxythiophene (EDOT, Aldrich) were used as received. Tetrabutylammonium perchlorate (TBAP, Fluka, >98%) was used after drying in a vacuum oven at 100 °C for 10 h. PEDOT films were electrochemically prepared on gold-on-silicon electrodes (with chromium adhesive layers, Inosteck) in an ACN solution containing 0.10 M TBAP and 0.030 M EDOT with an EG&G model 273 potentiostat−galvanostat. The gold-on-silicon electrodes were annealed for 5 min with a hydrogen flame prior to use as a working electrode after they had been rinsed thoroughly with methanol and deionized water. A platinum foil was used as a counter electrode and an Ag wire as a reference electrode. After electrochemical synthesis, the films were rinsed thoroughly with ACN to remove excess monomer, oligomers, and electrolyte molecules and dried under vacuum at room temperature.

Molecular Imaging's PicoSPM AFM with a current-sensing tip, CS-AFM, was used in a contact mode to simultaneously

* To whom correspondence should be addressed. Email: smpark@postech.edu. Phone: +82-54-279-2102. Fax: +82-54-279-3399.

10.1021/jp055791b CCC: $33.50
Published on Web 07/07/2006

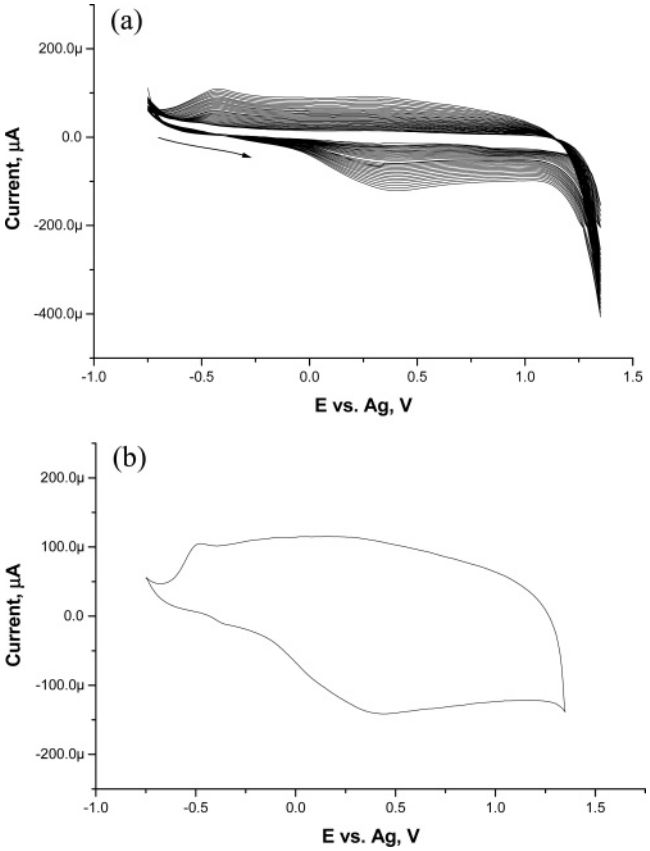

Figure 1. (a) A series of CVs recorded during the growth of the PEDOT film in ACN solution containing 0.03 and 0.1 M TBAP at a scan rate 100 mV/s (30 cycles) and (b) a typical cyclic voltammogram recorded for a PEDOT film in ACN without monomer molecules present.

obtain topographical and current images. The platinum/iridium-coated cantilevers (spring constant, ~0.16−0.41 N/m) were purchased from Nanosensors (http://www.nanosensors.com). The load force was maintained below 7 nN to avoid damages of the tip and the film. During the I/V measurement at a given spot of the film, a load force was always maintained at 7 nN. A bias voltage between the substrate (gold electrode) and the conducting cantilever (which is grounded) was 50 mV during all the imaging experiments. Before imaging the PEDOT film-covered surfaces, they were purged with the high purity nitrogen gas (99.999%, BOC Gases) to minimize the moisture and water, and all the AFM experiments were carried out under the controlled nitrogen atmospheric environment.

The UV−vis absorption spectra of PEDOT films were taken with an Oriel InstaSpec IV spectrometer with a charge-coupled device (CCD) array detector, which was configured in a near normal incidence reflectance mode by use of a bifurcated quartz optical fiber.[14c,16] The wavelength of the spectrograph was calibrated with a small mercury lamp. The reference spectrum was first taken from a clean bare gold-on-silicon electrode. A dried PEDOT-covered electrode was then placed at the end of the bifurcated optical fiber instead of the bare gold-on-silicon electrode, and the absorption spectrum of the film was recorded.

Results and Discussion

Figure 1a shows a series of cyclic voltammograms (CVs) obtained during the potentiodynamic growth of a PEDOT film in an ACN solution containing 0.10 M TBAP and 0.030 M EDOT. The film was grown by repeatedly cycling potentials between −0.75 and 1.35 V on the gold-on-silicon electrode.

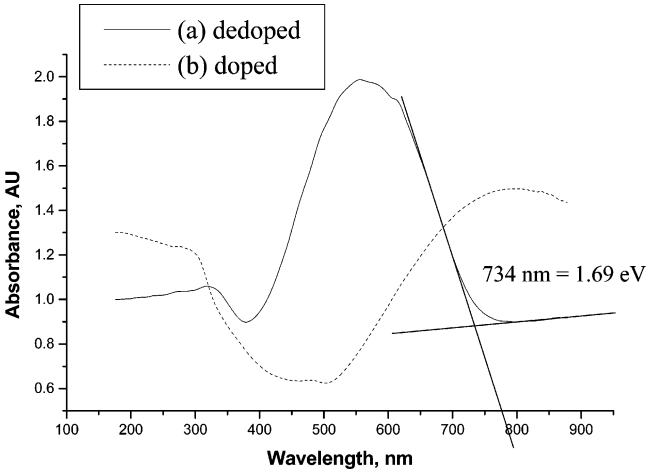

Figure 2. Absorption spectra recorded at the PEDOT films prepared by potentiodynamic method (30 cycles) and then dedoped at −0.8 V (a) and doped at 1.3 V (b) in the ACN solution containing 0.1 M TBAP.

The oxidation potential of the monomer EDOT is about 1.1 V (see Figure 1a) and the broad increasing peak currents of the PEDOT film with every potential cycle (Figure 1a) indicate a continuous growth of the film on the electrode surface. Figure 1b shows a CV recorded for a film prepared without monomer molecules present. These CVs showing broad redox peaks in the wide potential range are in good agreement with those reported in the literature.[7c,d] Since various interpretations of these oxidation peaks have been reported in the literature,[7b−d] we are not going to address the problem here.

Two absorption spectra obtained from a PEDOT film potentiodynamically grown (30 cycles) in 0.10 M TBAP and 0.030 M EDOT on the gold-on-silicon electrode are shown in Figure 2. The absorption spectra shown in Figure 2 were obtained after the film was rinsed thoroughly with ACN to remove excess monomer, oligomers, and electrolyte molecules and dedoped at −0.8 V for 300 s (a) and doped at 1.3 V (b), both in ACN containing just 0.10 M TBAP. The spectrum for the dedoped PEDOT film shows a broad absorption peak with a maximum at 580 nm corresponding to the $\pi-\pi^*$ transition (Figure 2a).[7a,d] When the PEDOT film is doped or oxidized, the maximum absorption peak is shifted to a longer wavelength at about 800 nm due to the formation of the radical cations and dications (Figure 2b).[7a,d]

Figure 3 shows topographic (a) and current (b) images simultaneously obtained for the identical surface of $3 \times 3\ \mu m^2$ of a PEDOT film, which was completely dedoped at −0.80 V for 300 s. The thickness of the film examined here was estimated to be 108 nm. The current image shown in Figure 3b, which was obtained at a 50 mV bias voltage between the substrate and the tip, shows bright (high current-flowing) and dark (low current-flowing) regions. The dedoped PEDOT film, which would be in an electrically neutral or insulating state, still shows conductive spots (bright regions) as shown in Figure 3b. I/V curves were obtained to evaluate the electrical properties of the film at 25 points labeled in Figure 3, but only three typical results obtained from points A, M, and Y across the diagonal line are shown in Figure 4 as I/V curves obtained at other points were very similar. The measurements were made between the probe and the substrate electrode by scanning the voltage between −3.0 and +3.0 V. The differences in shapes for these I/V curves result from the inhomogeneity of the polymer film as reported in the literature.[14b] In Figure 4, the I/V curves show the behaviors of typical semiconductors. Alperson et al. assigned band gaps of CdSe Q-dots from zero current gaps in I/V curves

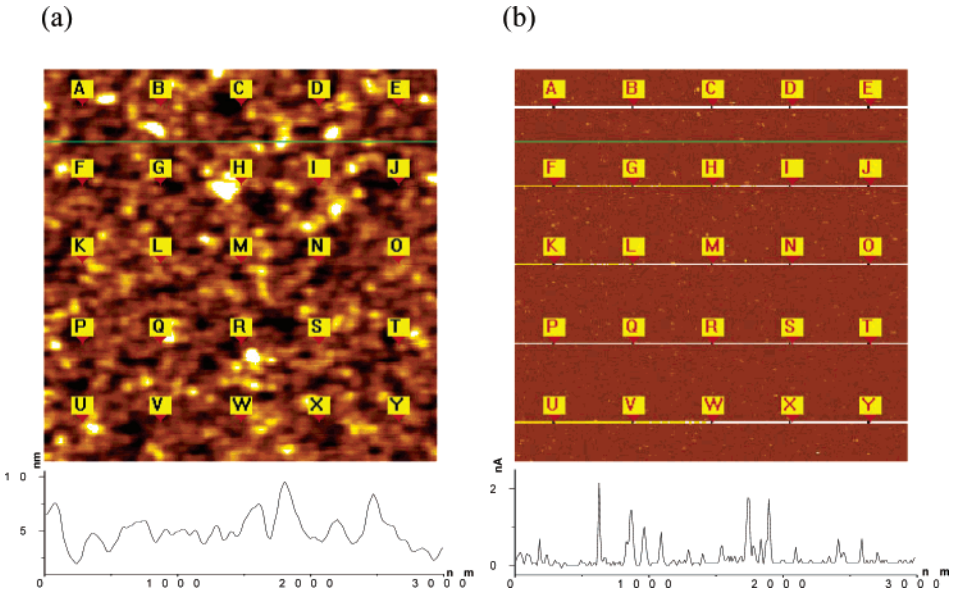

Figure 3. Topographic (left) and current (right) images ($3 \times 3\ \mu m^2$) with their cross-sectional analyses for the PEDOT film prepared by potentiodynamic method (30 cycles) and dedoped at −0.8 V for 300 s.

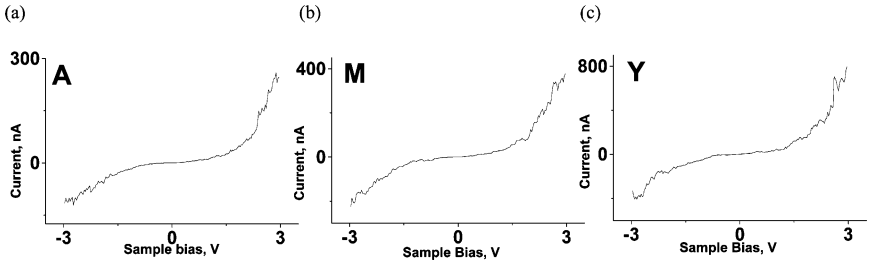

Figure 4. I/V curves obtained from points A (a), M (b), and Y (c) in Figure 3b.

by CS-AFM.[12] By treating the PEDOT film in the same manner as they did, we can correlate the band gaps obtained from electrical and optical measurements. Two representative dI/dV signals shown in Figure 5 were obtained from the I/V traces recorded at spots G and Q marked in Figure 3b (not shown) to identify the band gap, which is 2.28 eV (Figure 5a) and 1.59 eV (Figure 5b). The gaps obtained from the I/V curves were different depending on the spots, at which they were measured because the doping levels are all different at these spots.

The absorption spectrum shown in Figure 2 is an ensemble average of optical properties of the whole PEDOT film within the area where the probing beam passed through, and, therefore, each I/V curve measured at a specific point cannot represent all I/V characteristics in the PEDOT surface. Thus, I/V curves were obtained at randomly selected 500 points and then were averaged to give a curve shown in Figure 6a in order to see how the band gaps obtained from the I/V curves and the absorption edge in the absorption spectrum are related with each other. We drew two lines, one along the falling edge of the absorption band and the other along the background of the spectrum, in Figure 2a to determine the absorption edge, which is 1.69 eV or 734 nm for the neutral PEDOT film. The dI/dV signal shown in Figure 6b was obtained from the average I/V curve of 500 curves, which is shown in Figure 6a. The band gap estimated from the distance between two small first peaks in the negative and positive voltage regions is about 1.75 eV. The band gaps determined by two different methods are in excellent agreement with each other. Our results indicate that the PEDOT film is inhomogeneous although the average band gap obtained from the electrical measurements can be said to be in good agreement with that obtained by the optical method.

In the dI/dV curve shown in Figure 6b, we see that the dI/dV values are not 0 even within the band gap region of the potential axis. This is because the average current shown in Figure 6a was obtained from the currents flowing in both conductive and nonconductive spots, and thus, the residual current flow is significant even in the band gap region. This phenomenon is also observed in the absorption spectrum as well (Figure 2), where significant absorption is observed even below the band gap energy where no band gap transition should take place. Unless one deals with a single crystal semiconductor, the phenomenon like these is usually observed because the property measured is ensemble averaged within the area probed.

Figure 7 shows topographic (a) and current (b) images obtained simultaneously for the surface of a PEDOT film potentiodynamically grown (30 cycles) and then doped at +1.30 V in an ACN solution containing 0.10 M TBAP. The current image shown in Figure 7b, which was obtained at a 50-mV bias voltage, also shows bright (high current-flowing) and dark (low current-flowing) regions. The vertical conductivities of the film between the tip and the substrate electrode were calculated by using the contact area of the tip with the polymer employing the Hertz theory,[14b−e,17] and the average conductance values were obtained from the cross sectional analyses of the current images shown below the dedoped (Figure 3b) and the doped (Figure 7b) PEDOT films. The contact area between the tip and the sample was calculated to be 38.7 nm^2 under our experimental conditions, assuming Poisson's ratio of PEDOT to be 0.38 just as for platinum and Young's modulus of all PEDOT films of 3.2 GPa, which is the same as that for the

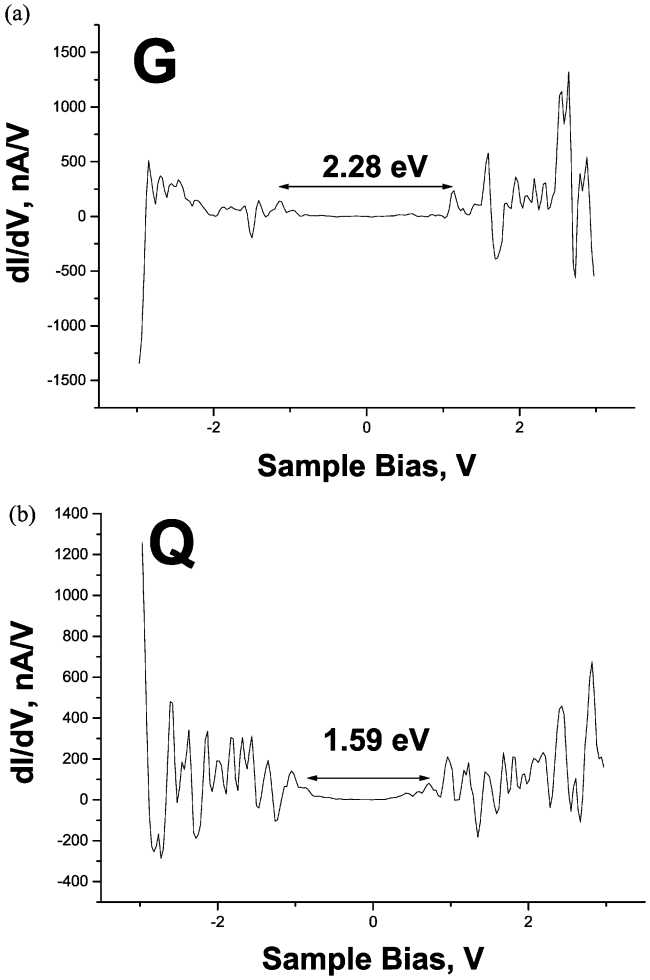

Figure 5. dI/dV signals obtained from curves recorded at spots G (a) and Q (b) in Figure 3b.

PEDOT nanofiber.[18] The conductivity was then calculated from

$$\sigma = \frac{1}{R} \cdot \frac{l}{A} \tag{1}$$

where σ is the conductivity, R the resistance calculated from the current and the bias potential, A the contact area calculated from the Hertz theory along with appropriate constants described above, and l the thickness of the film obtained from the cross-sectional view of the scanning electron microscopic image. While one may raise a question of whether the conductivity thus obtained would be valid due to a much larger contact area on the other side of the film than that of the tip contact, it has been customary to use the tip contact area for conductivity calculation in the CS-AFM measurements as the tip limits the electrical current flow. When the PEDOT film was doped, it showed much more conductive white regions than the dedoped one did, and an average conductivity of 269 S/cm was obtained for the film shown in Figure 7b while 0.11 S/cm was obtained for the dedoped film shown in Figure 3b.

Figure 8 shows three typical I/V curves recorded from the doped PEDOT film at points A, M, and Y shown in Figure 7b. The curves are more linear and higher currents flow than on the film shown in Figure 4. The doped PEDOT film acts more like a resistor than a semiconductor. An average I/V curve could not be obtained for the doped film in this case because of the current saturation (current limit: 1000 nA) observed during the current measurements and, thus, only two representative dI/dV signals shown in parts a and b of Figure 9 were taken from

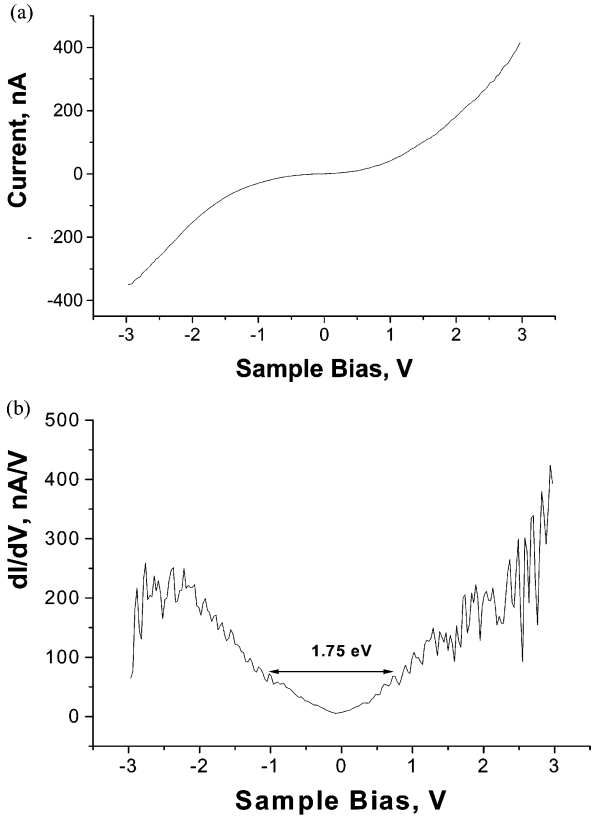

Figure 6. (a) I/V curve by averaging I/V curves at randomly selected 500 points and (b) dI/dV signal of the curve in (a).

points D and V. Both these I/V curves show an inflection point near V = 0 V (not shown). The d*I*/d*V* signal of linear I/V curves such as that from point A shown in Figure 8 displayed no change in slope (not shown), because its I/V behavior resembles that of a resistor. The distance between two peaks in the dI/dV curve shown in Figure 9 was about 0.15 eV for the doped PEDOT film, which shows a metallic property with almost zero band gap even for relatively less conducting films. One can also see in Figure 9 that there are many states between the wider band gap marked by two high dI/dV peaks, depending on the doping level of the film. The absorption maximum of the doped PEDOT was reported to be about 0.5 eV;[7a] it is thus certain that the absorption edge is close to 0 eV when estimated in the same way as was done for the spectrum shown in Figure 4a.

Figure 10 shows the effects of the film thickness on topographic (top) and current (bottom) images when the films were potentiodynamically grown for (a) 15 and (b) 45 cycles and then doped at +1.3 V until no further anodic currents flowed. The images of PEDOT grown for 30 cycles shown in Figure 7 should be between the two shown in parts a and b of Figure 10. Conductivities calculated from cross-sectional analyses at current images are 75.6, 269, and 990 S/cm, respectively, for the films shown in Figures 10a, 7, and 10b; these results indicate that conductivities increase roughly in a quadratic order as the film thickness increases. This trend was reproducible, although the exact values of conductivities were not exactly reproduced.

According to eq 1, the conductivity (σ) should stay constant provided that the resistance (R) is directly proportional to the film thickness, l, as is usually the case. The conductivity increased as the polymer became thicker in our case, indicating that the resistance actually decreased as the film thickness increased. This rather unusual phenomenon is often observed for conducting polymer films until the thickness reaches a certain

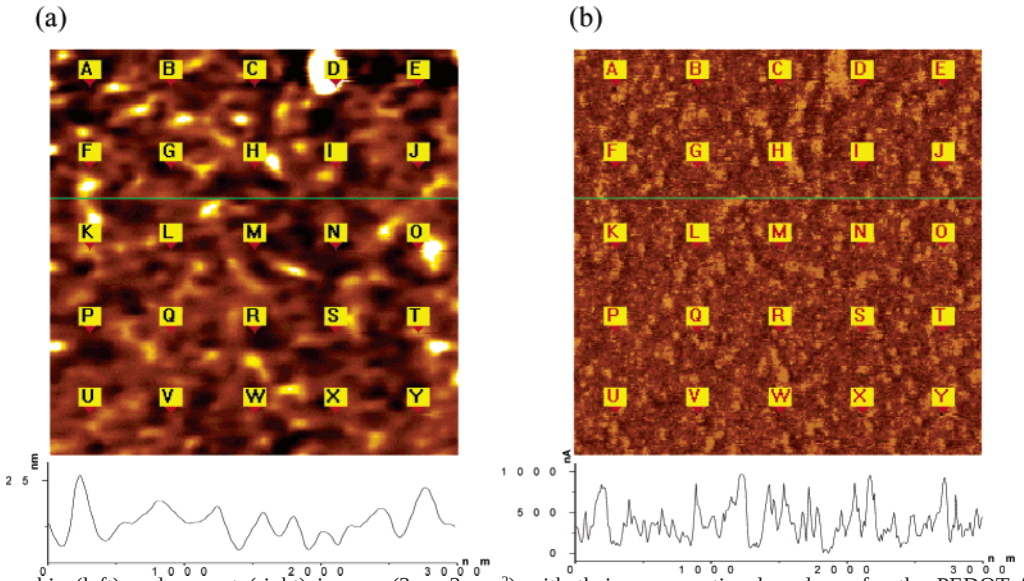

Figure 7. Topographic (left) and current (right) images (3 × 3 μm^2) with their cross-sectional analyses for the PEDOT film prepared by potentiodynamic method (30 cycles) and doped at 1.3 V until no further currents flow.

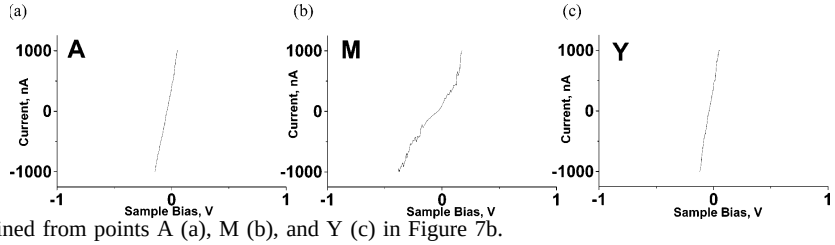

Figure 8. I/V curves obtained from points A (a), M (b), and Y (c) in Figure 7b.

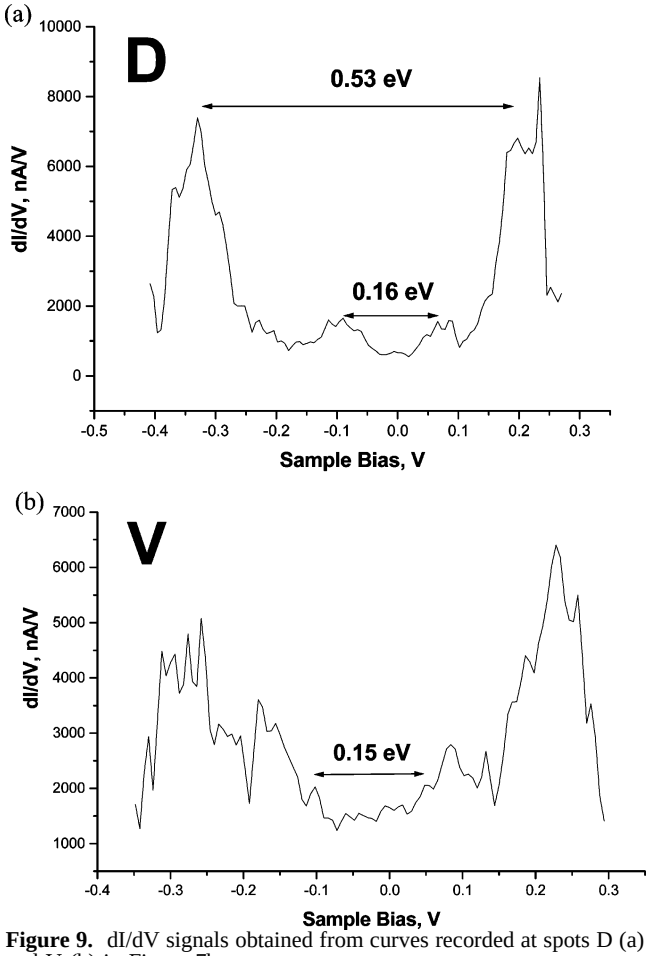

Figure 9. dI/dV signals obtained from curves recorded at spots D (a) and V (b) in Figure 7b.

level and then decreases upon further increase in thickness.[14d,15e] In an earlier phase of the film growth, the conductivity is always much lower than expected because of the short chain lengths of primarily oligomers and a larger fraction of degradation products due to competing reactions to overoxidized polymers. As the film grows, more extensive conjugation is obtained across the longer chains with the relative fraction of degradation products decreased and the relative conductivity increased.

Depending on an applied current during the galvanostatic growth, a different overpotential is imposed to the electrode during the polymerization reaction and the conductivities of PEDOT films may vary accordingly. We thus examined effects of the current density as well as the applied potential.

The PEDOT films were prepared using an identical anodic charge density of 23.8 mC/cm^2 by applying: 0.05 mA for 200 s (a), 0.2 mA for 50 s (b), and 1.0 mA for 10 s (c). The overpotentials measured in the steady state during these experiments were measured to be 1.20, 1.31, and 1.43 V, respectively, for the above applied currents. The average conductivities calculated from the average current profiles were 525, 1420, and 1635 S/cm, respectively, for these films. These results indicate that a more conductive film is obtained when a higher current is used for the reaction even though exactly the same amount of anodic charge is used. These results are in good agreement with our recent observations made during the polypyrrole growth.[14e] As reported in the literature,[6] conductivities of 500−700 S/ cm for PEDOT are easily obtained, which can be raised to a conductivity of 1000 S/cm or higher if processing conditions are well controlled. The conductivities of the PEDOT films shown here demonstrate that this would be the case and their conductivities are comparable with those of polypyrrole but higher than those obtained from polyaniline.[14b−e] The root-mean-square (RMS) roughness was

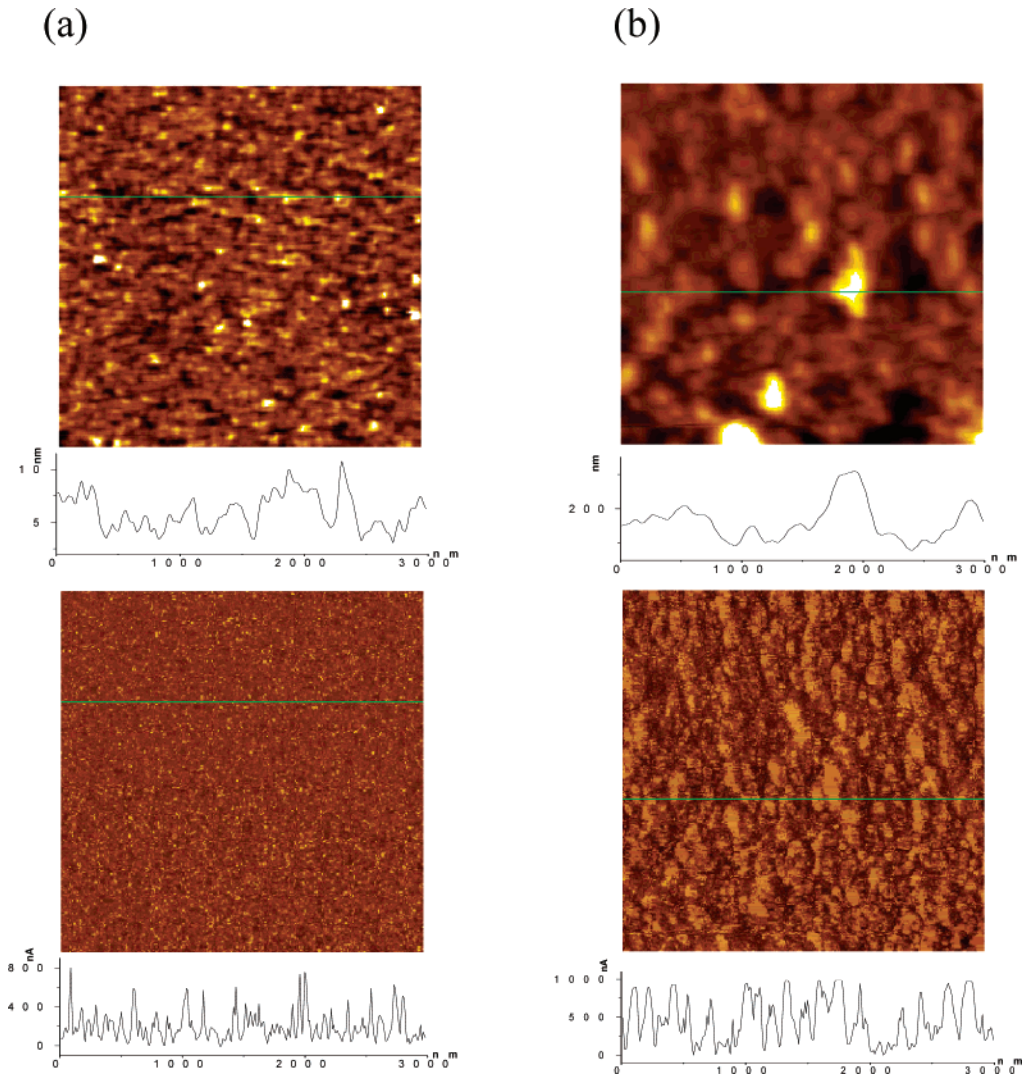

Figure 10. Topographic (top) and current (bottom) images ($3 \times 3\ \mu m^2$) with their cross-sectional analyses for the PEDOT films potentiodynamically grown for (a) 15 and (b) 45 cycles and then doped at 1.3 V until no further currents flow.

5.5, 38.2, and 65.0 nm for these films, respectively, which indicates the current density also affects the morphology of the PEDOT film surface. High current densities used during the film preparation make the surfaces rougher and the topographic images (not shown) are not clearly defined.

The effect of another parameter, i.e., the applied potential during the potentiostatic growth was evaluated in determining the quality of the film. The film thicknesses measured by scanning electron microscope were 117, 103, 332 nm, respectively, when the films were prepared at 1.25 V for 120 s (a), 1.35 V for 30s (b), and 1.40 V for 30 s (c). Thus the thickness of the PEDOT film prepared at a relatively lower oxidation potential of 1.25 V for 120 s is very close to that of the film prepared at 1.35 V for 30 s, but the area of the current flowing regions in the current image (not shown) for film b was significantly larger than that for film a with the RMS roughness (16.3 nm) also significantly higher than that for film a (1.3 nm) in the topographic images. The film prepared at 1.4 V for 30 s show the highest conductivity in the current image as well as the highest roughness in the topographic image (not shown). These results are in good agreement with those reported in the literature.[14e]

Our results here indicate that a thicker PEDOT film is preferred for higher film conductivity. Also, a more conductive film is obtained at a higher potential applied to the electrode during the preparation. This is probably because the oxidation potential of PEDOT is much higher than those of most other conducting polymers, although its oxidation potential range is very wide (Figure 1b). For conducing polymer films, the conductivity should be constant regardless of its thickness. However, the thicker PEDOT films turned out more conductive than thinner ones due perhaps to different chain lengths and different fractions of degradation products contained in the films of different thicknesses.

Conclusions

We have demonstrated in this study that: (1) the average band gap obtained from I/V curves are in excellent agreement with those obtained from the absorption spectra and (2) morphological and electrical properties of PEDOT films were affected by experimental parameters used during their preparation regardless of the type of the preparation methods. The PEDOT films act like band gap semiconductors in their neutral state, and the average band gap obtained from the peak-to-peak voltage differences of dI/dV curves is very close to the absorption edge obtained from the spectrum. Though conducting polymers behave like a semiconductor, we should not overlook their inhomogeneity; the surface of the conducting polymer has wide current distributions, and the current−voltage curves measured at different points in the current images are diverse.

The morphological and electrical properties of PEDOT films are very sensitive to the experimental conditions such as preparation methods, solvents, and electrolytes; thus, it is very important to control the experimental conditions to obtain a better-defined PEDOT film.

A merit of a conducting polymer may sometimes be its demerit because an advantage of diverse electrical properties can become a disadvantage of easily changing properties depending on experimental parameters. Only a complete understanding of their properties would allow us to tune their properties for better applications.

Acknowledgment. This work was supported by the SRC/ERC program of MOST/KOSEF (Grant No. R11-2000-070-06001-0), and the stipends for the graduate assistants were supplied by the BK21 program of the Korea Research Foundation.

References and Notes

(1) (a) Yu, G.; Gao, J.; Hummelen, J. C.; Wudl, F.; Heeger, A. J. *Science* **1995**, *270*, 1789. (b) Horowitz, G. *Adv. Mater.* **1998**, *10*, 365. (c) Kraft, A.; Grimsdale, A. C.; Holmes, A. B. *Angew. Chem., Int. Ed. Engl.* **1998**, *37*, 402. (d) Huitema, H. E. A.; Gelinck, G. H.; van der Putten, J. B. P. H.; Kuijk, K. E.; Hart, C. M.; Cantatore, E.; Herwig, P. T.; van Breemen, A. J. J. M.; de Leeuw, D. M. *Nature* **2001**, *414*, 599. (e) DeLongchamp, D.; Hammond, P. T. *Adv. Mater.* **2001**, *13*, 1455. (f) Dimitrakopoulos, C. D.; Malenfant, P. R. L. *Adv. Mater.* **2002**, *14*, 999. (g) Huynh, W. U.; Dittmer, J. J.; Alivisatos, A. P. *Science* **2002**, *295*, 2425. (h) Sun, B.; Marx, E.; Greenham, N. C. *Nano Lett.* **2003**, *3*, 961. (i) Argun, A. A.; Cirpan, A.; Reynolds, J. R. *Adv. Mater.* **2003**, *15*, 1338.

(2) Chen, G.; Guan, Z.; Chen, C. T.; Fu, L.; Sundaresan, V.; Arnold, F. H. *Nat. Biotechnol.* **1997**, *15*, 354. (b) Hagleitner, C.; Hierlemann, A.; Lange, D.; Kummer, A.; Kerness, N.; Brand, O.; Baltes, H. *Nature* **2001**, *414*, 293.

(3) Wessling, B. *Adv. Mater.* **1994**, *6*, 226.

(4) Smela, E. *Adv. Mater.* **2003**, *15*, 481.

(5) Groenendaal, L. B.; Jonas, F.; Freitag, D.; Pielartzik, H.; Reynolds, J. R. *Adv. Mater.* **2000**, *12*, 481.

(6) Kirchmeyer, S.; Reuter, K. *J. Mater. Chem.* **2005**, *15*, 2077.

(7) Pei, Q.; Zuccarello, G.; Ahlskog, M.; Inganäs, O. *Polymer* **1994**, *35*, 1347. (b) Chen, X.; Inganäs, O. *J. Phys. Chem.* **1996**, *100*, 15202. (c) Garreau, S.; Louarn, G.; Buisson, J. P.; Froyer, G.; Lefrant, S. *Macromolecules* **1999**, *32*, 6807. (d) Kvarnstrom, C.; Neugebauer, H.; Blomquist, S.; Ahonen, H. J.; Kankare, J.; Ivaska, A. *Electrochim. Acta* **1999**, *44*, 2739.

(8) Cui, X. D.; Primak, A.; Zarate, X.; Tomfohr, J.; Sankey, O. F.; Moore, A. L.; Moore, T. A.; Gust, D.; Harris, G.; Lindsay, S. M. *Science* **2001**, *294*, 571. (b) Cui, X. D.; Primak, A.; Zarate, X.; Tomfohr, J.; Sankey, O. F.; Moore, A. L.; Moore, T. A.; Gust, D.; Nagahara, L. A.; Lindsay, S. M. *J. Phys. Chem. B* **2002**, *106*, 8609.

(9) Zhao, J.; Davis, J. J.; Sansom, M. S. P.; Hung, A. *J. Am. Chem. Soc.* **2004**, *126*, 5601. (b) Cai, L.; Tabata, H.; Kawai, T. *Nanotechnology* **2001**, *12*, 211.

(10) Dai, H.; Wong, E. W.; Lieber, C. M. *Science* **1996**, *272*, 523. (b) de Pablo, P. J.; Gomez-Navarro, C.; Martinez, M. T.; Benito, A. M.; Maser, W. K.; Colchero, J.; Gomez-Herrero, J.; Baro, A. M. *Appl. Phys. Lett.* **2002**, *80*, 1462. (c) Li, J.; Stevens, R.; Delzeit, L.; Tee Ng, H.; Cassell, A.; Han, J.; Meyyappan, M. *Appl. Phys. Lett.* **2002**, *81*, 910.

(11) Sakaguchi, H.; Hirai, A.; Iwata, F.; Sasaki, A.; Nagamura, T.; Kawata, E.; Nakabayashi, S. *Appl. Phys. Lett.* **2001**, *79*, 3708. (b) Wold, D. J.; Haag, R.; Rampi, M. A.; Frisbie, C. D. *J. Phys. Chem. B* **2002**, *106*, 2813. (c) Beebe, J. M.; Engelkes, V. B.; Miller, L. L.; Frisbie, C. D. *J. Am. Chem. Soc.* **2002**, *124*, 11268.

(12) Alperson, B.; Cohen, S.; Rubinstein, I.; Hodes, G. *Phys. Rev. B* **1995**, *52*, R17017. (b) Alperson, B.; Rubinstein, I.; Hodes, G. *Phys. Rev. B* **2001**, *63*, 081303.

(13) Loiacono, M. J.; Granstrom, E. L.; Frisbie, C. D. *J. Phys. Chem. B* **1998**, *102*, 1679. (b) Park, W. I.; Yi, G.-C.; Kim, J.-W.; Park, S.-M. *Appl. Phys. Lett.* **2003**, *82*, 4358. (c) Tivanski, A. V.; Bemis, J. E.; Akhremitchev, B. B.; Liu, H.; Walker, G. C. *Langmuir* **2003**, *19*, 1929.

(14) Lee, H. J.; Park, S.-M. *J. Phys. Chem. B* **2004**, *108*, 1590. (b) Han, D.-H.; Park, S.-M. *J. Phys. Chem. B* **2004**, *108*, 13921. (c) Lee, H. J.; Park, S.-M. *J. Phys. Chem. B* **2004**, *108*, 16365. (d) Lee, H. J.; Park, S.-M. *J. Phys. Chem. B* **2005**, *109*, 13247. (e) Han, D.-H.; Lee, H. J.; Park, S.-M. *Electrochim. Acta* **2005**, *50*, 3085. (f) Park, S.-M.; Lee, H. J. *Bull. Korean Chem. Soc.* **2005**, *26*, 697. (g) Hong, S.-Y.; Jung, Y. M.; Kim, S. B.; Park, S.-M. *J. Phys. Chem. B* **2005**, *109*, 3844.

(15) Planes, J.; Houze, F.; Chretien, P.; Schneegans, O. *Appl. Phys. Lett.* **2001**, *79*, 2993. (b) Park, J. G.; Lee, S. H.; Kim, B.; Park, Y. W. *Appl. Phys. Lett.* **2002**, *81*, 4625. (c) Saha, S. K.; Su, Y. K.; Lin, C. L.; Jaw, D. W. *Nanotechnology* **2004**, *15*, 66. (d) Ionescu-Zanetti, C.; Mechler, A.; Carter, S. A.; Lal, R. *Adv. Mater.* **2004**, *16*, 385. (e) Wu, C. G.; Chang, S. S. *J. Phys. Chem. B* **2005**, *109*, 825.

(16) Pyun, C.-H.; Park, S.-M. *Anal. Chem.* **1986**, *58*, 251. (b) Zhang, C.; Park, S.-M. *Anal. Chem.* **1988**, *60*, 1639. (c) Zhang, C.; Park, S.-M. *Bull. Korean Chem. Soc.* **1989**, *10*, 302.

(17) Isrraelachvili, J. *Intermolecular and Surface Forces*, Academic Press: London, 1992. (b) Riedo, E.; Brune, H. *Appl. Phys. Lett.* **2003**, *83*, 1986.

(18) Duvail, J. L.; Rétho, P.; Godon, C.; Marhic, C.; Louarn, G.; Chauvet, O.; Cuenot, S.; Nylsten, B.; Dauginer-De Pra, L.; Demoustier-Chempagne, S. *Synth. Met.* **2003**, *135*−*136*, 329.